Improved volatile cargo retention and mechanical properties of capsules via sediment-free in situ polymerization with cross-linked poly(vinyl alcohol) as an emulsifier ϙ

Yan Zhang [a,b], Abdullah Naseer Mustapha [a,b], Xiaotong Zhang [b], Daniele Baiocco [b], Gilmore Wellio [a,b], Thomas Davies [c], Zhibing Zhang [b,⇑], Yongliang Li [a,⇑]

[a] Birmingham Centre for Energy Storage (BCES), School of Chemical Engineering, University of Birmingham, Edgbaston, Birmingham, West Midlands B15 2TT, United Kingdom

[b] Micromanipulation and Microencapsulation Research Group (MCAP), School of Chemical Engineering, University of Birmingham, Edgbaston, Birmingham, West Midlands B15 2TT, United Kingdom

[c] Cardiff Catalysis Institute, School of Chemistry, Cardiff University, Cardiff, Wales CF10 3AT, United Kingdom

graphical abstract

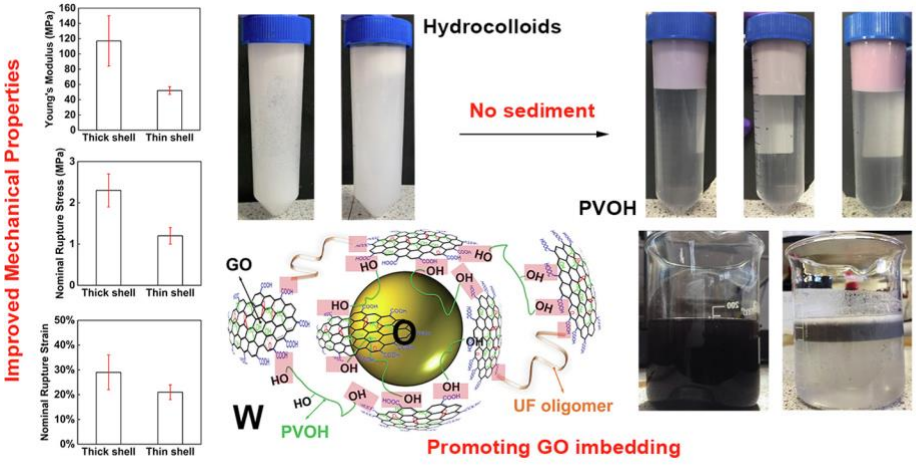

article info

abstract

Hypothesis: It is hypothesized that poly(vinyl alcohol) (PVOH) as an emulsifier destabilizes the insoluble molecular aggregates by increasing interparticle interactions and their tendency toward agglomeration into large particle aggregates during the encapsulation process of one-step in situ polymerization. Porosity of capsule shells is expected to decrease with reducing agglomeration tendency to allow dense packing of smaller insoluble aggregates. Cross-linking the polymer network further reduces shell perme-ability to improve the retention of volatile cargos. PVOH also modifies the short-range order of polymer

ϙ The First Author gave a Young Investigator Perspective oral presentation at the 9th International Colloids Conference, 16–19 June 2019, Sitges, Barcelona, Spain.

⇑ Corresponding authors at: Birmingham Centre for Energy Storage (BCES), School of Chemical Engineering, University of Birmingham, Edgbaston, Birmingham, West Midlands B15 2TT, United Kingdom (Y. Li); Micromanipulation and Microencapsulation Research Group (MCAP), School of Chemical Engineering, University of Birmingham, Edgbaston, Birmingham, West Midlands B15 2TT, United Kingdom (Z. Zhang).

E-mail addresses: z.zhang@bham.ac.uk (Z. Zhang), y.li.1@bham.ac.uk (Y. Li).

Keywords:
Capsule
Emulsifier
Graphene oxide
Poly(vinyl alcohol)
Sediment
Volatile

network to bestow improved mechanical properties in addition to the shell thickening effect at appropri-ate synthesis conditions.

Experiments: PVOH was used to stabilize a heptane-in-water emulsion as a template for producing cap-sules via one-step in situ polymerization. Shell morphologies at different PVOH concentrations were compared. Physical freeze-thawing and chemical cross-linking were adopted separately to synthesize capsules with a volatile cargo, and its retention was characterized qualitatively by a solvatochromism-based fluorescent method and quantitative payload calculation. Mechanical properties of capsules were tested with micromanipulation. The effect of graphene oxide (GO) impregnation into capsules was stud-ied with various co-emulsifiers.

Findings: When PVOH alone was used as the emulsifier for capsule synthesis, the higher its concentra-tion, the more porous the shell structure was. At very low concentrations, visible pores were eliminated. Freeze-thaw cycles reduced the permeability of capsule shells when visible pores were absent. Chemical cross-linking with poly(acrylic acid) (PAA) significantly improved the retention of volatile cargo heptane. PVOH substantially reduced polymer sediment during capsule synthesis, which eliminated the tedious centrifugation procedure that normally would have followed. Superior mechanical strength of capsules was achieved with PAA cross-linked PVOH at appropriate conditions. The impregnation of aqueously dis-persed GO into capsules was also promoted by using PVOH but not hydrocolloid emulsifiers.

1. Introduction

Encapsulation and full retention of volatile, small molecular weight active ingredients is a challenging task that remains unsolved by current technologies used in industry and academia, as most typical microcapsule membranes are highly permeable [1]. It is, however, very important in a wide range of areas such as personal/home care products, pharmaceuticals, foods, etc. In particular, microencapsulation of solid–liquid phase change mate-rials (PCMs) has been recognized as a vital technology to protect them from leakage and running off and thus received tremendous attention from fundamental studies to industrial development in recent decades [2]. For cold thermal energy storage applications, PCMs with appropriate liquid-solid phase transition temperatures normally have high vapor pressure and low boiling points, making their encapsulation even more challenging than other applications for full retention.

Among all currently available encapsulation techniques, in situ polymerization is believed to be the most suitable method for retaining volatile PCMs due to its dense polymer structure network to prevent leakage and achieve long-term retention [3]. In situ polymerization is a widely used industrial method to synthesize amino resin capsules for the paper industry [4], self-healing mate-rials [5–7], and thermal energy storage [8,9] to name a few. Such an encapsulation technique utilizes an oil-in-water (O/W) emul-sion as a template and cross-links water soluble monomers to pro-duce precipitates, which deposit on the O/W interface to form polymer films encaging the oil droplets to form capsules eventually [10,11]. Produced polymer precipitates not only can deposit on the O/W interface but also can disperse excessively in the aqueous phase as a side product. In case of the latter, multiple rounds of centrifugation and separation procedures are required to harvest the final capsule products, which is time-consuming and tedious. In addition, if the oil phase has a higher density than water, both capsules and precipitates would become sediment after centrifuga-tion, posing difficulty to separate them.

In our previous work of screening emulsifiers for retaining vola-tile PCMs [3], we tested poly(vinyl alcohol) (PVOH) as the emulsi-fier, and the preliminary result was unsuccessful. In this work, we furthered the preliminary study of using PVOH to synthesize cap-sules and discovered some very interesting and attractive merits of such an emulsifier. Firstly, PVOH did not seem to produce sedi-ment during encapsulation. This eliminates the tedious repetitive routine of centrifugation and resolved the issues mentioned above. Secondly, the mechanical properties of capsules produced with PVOH were superior to those synthesized with hydrocolloids. Last but not least, impregnation of graphene oxide (GO) from the aque-ous phase into capsules appears to be effective at the presence of PVOH. In order to employ such advantages of PVOH in this work, we investigate various methods to enhance the barrier property for retention of the volatile heptane cargo. Our successful effort to improve the shell barrier properties makes PVOH a potential advantageous emulsifier candidate for capsule production via one-step in situ polymerization.

2. Materials and methods

2.1. Materials

The following materials were purchased from Sigma-Aldrich UK: poly(vinyl alcohol) (363170, M_W 13,000–23,000, 87–89% hydrolysed), poly(acrylic acid) (306215, average M_V ~ 1,250,000), gelatin from porcine skin (48722), xanthan gum from Xan-thomonas campestris (Sigma-Aldrich G1253), methyl cellulose (Sigma-Aldrich M0262, viscosity 400 cP), urea (U5128, ACS reagent grade 99.0–100.5%), resorcinol (398047, ACS reagent, 99.0%), ammonium chloride (A9434, for molecular biology, 99.5%), formaldehyde (47608, for molecular biology, BioReagent, 36.0% in H_2O), Nile red (72485), heptane (246654, anhydrous, 99%), and graphene oxide (GO) nanocolloids (795534, 2 mg/mL, dispersion in H_2O).

2.2. Capsule synthesis

Detailed capsule synthesis was performed according to our standard protocol published elsewhere [12,13]. To sum up, the aqueous phase was prepared by dissolving the emulsifier first at an appropriate concentration into 150 g deionized water, followed by dissolving 2.50 g urea, 0.25 g resorcinol and 0.25 g NH_4Cl. Gela-tin was dissolved by heating up to 50 LC and then maintained at the temperature under stirring for 5 min, then cooled down natu-rally. Methyl cellulose and xanthan gum were dissolved using high shear homogenization at 3000 rpm for 5 min and ultrasonication for 5 min for degassing air bubbles. For capsules prepared by pure PVOH, the emulsifier solution was prepared by dissolving the poly-mer in deionized water at 90 LC for 4 h. For freeze-thawing, the emulsifier solution was frozen at 20 LC for 16 h, and then thawed at 20 LC for 8 h. 5 of such freeze–thaw cycles were carried out before capsule synthesis. When chemical cross-linking with PAA was required, 0.01 wt% PVOH and 0.01 wt% PAA were dissolved

at 90 LC for 4 h and 12 h respectively and cooled down in air. When synthesizing capsules with GO, 5 mL GO nanocolloid was added into the prepared emulsifier solution. The pH of all prepared solu-tions was adjusted to 3.5 with HCl. When fluorescent sensing was required, Nile red was dissolved in heptane via ultrasonication for 10 min prior to emulsification. Otherwise, heptane without fluo-rescent staining was emulsified in the aqueous phase inside a glass beaker on a Silverson high shear homogenizer at 1200 rpm for 20 min. The produced emulsion was then transferred into a 250 mL jacketed beaker connected to a water bath, and maintained under agitation at 600 rpm on a mechanical stirrer at 20 LC. 6.5 mL formaldehyde was injected into the emulsion and the beaker open-ing was covered with Al foil. The polymerization was initiated by heating up the circulating water to 55 LC and maintained at this temperature for 4 h. The final products were then centrifuged and vacuum filtered.

2.3. Characterization

2.3.1. Bright-field and fluorescent microscopy

Optical microscopy images were taken on a Leica DMRBE microscope with Motic Images Advanced 3.2 software. The fluores-cent color of capsules under excitation was investigated on the same microscope with a CoolLED pE-300 illumination system. A H3 filter cube (BP420-490), a dichromatic mirror (510) and a sup-pression filter (LP 515) were applied. The blue excitation light max-imum was around 460 nm.

2.3.2. Scanning electron microscopy

The morphological properties and shell thickness of the micro-capsules were characterised using a Hitachi TM3030 Plus table-top SEM. The samples were coated with 5 nm of gold, using a Quorum Q150R ES gold sputtering machine, with a pressure of 0.5 bar, and argon as the inert gas. Where shell thickness was characterized, capsules were firstly crushed with liquid nitrogen and imaged on SEM subsequently. For each thickness characterization, 10 ran-domly selected capsules were used and each capsule was mea-sured at 10 different locations.

2.3.3. X-ray diffraction

A Bruker D8 Advanced diffractometer with a Cu tube (1.5418 Å) and LYNXEYE detector was used under ambient conditions. The powders were loaded into a circular PMMA specimen holder load-ing terminal, and the measurement data were collected in a range of 2h = 5–65L, with a scanning rate of 0.8 s per step and an angular increment of 0.01L.

2.3.4. Micromanipulation

A self-built micromanipulation system with a CCD camera was used for characterizing the mechanical properties of capsules. Details for the system configuration are described elsewhere [14]. Force transducers 403A and 405A (Aurora Scientific Inc., Canada) were mounted with polished glass needles. Capsules in a sample were dispensed via a pipette onto a pre-cut glass substrate which was fitted onto the system, and then dried to achieve disper-sion. System compliance was tested 5 times and the mean value was used to compensate the force transducer and stage displace-ments. 30 randomly selected capsules were compressed until either they broke or the maximum displacement load was reached.

2.3.5. Payload and tableting

Capsule payload was characterized as follows: capsules were freshly dried and weighed. The powder weight was monitored every 24 h for the following 4 d. The powder sample was after-wards pressed into a tablet with a punch die on a Lloyd X mechan-ical tester (LS100 Plus) with a loading capacity of 100 kN. The samples were tableted at 10 mm/min to 80 kN and held at this load for 120 s, and then the force was relieved. The weight of the final tablet was recorded and the payload was calculated as (capsule weight – tablet weight)/capsule weight. Tablet samples were also prepared in this way for Raman microscopy.

2.3.6. Raman microscopy

Raman spectra of samples were collected on a Renishaw inVia Qontor confocal Raman microscope with a RL785 (785 nm) diode laser and a CCD detector. Three accumulations were completed for each scan to reduce the noise-to-signal ratio. A 5 objective was used for the pure GO and GO embedded capsules, with 0.5% and 0.1% laser power respectively. For the non-GO embedded cap-sules, a 20 objective was used with 10% laser power.

2.3.7. Transmission electron microscopy

Transmission electron microscopy (TEM) was performed on a JEOL JEM-2100 operating at 200 kV. TEM samples were prepared as follows: a small amount of capsule sample was mixed with LR White resin in an Eppendorf tube overnight at 60 LC until the resin set. Molded samples were sectioned using a Reichert Jung Ultra microtome and slices approx.100 nm thick were placed onto car-bon/formvar coated Cu grids. Multiple areas were analysed for each sample.

3. Results and discussion

For this application, we have screened hundreds of organic chemicals with the following criteria: (1) a boiling point no lower than 90 LC; (2) a freeze point no higher than – 90 LC; (3) large enthalpy of fusion. Among all shortlisted candidates, heptane was selected as the model PCM due to its low cost and ease of com-mercial availability.

3.1. Encapsulation with pristine PVOH

Since hydroxyls can react with methylol urea [15], PVOH should theoretically favor capsule formation even if not retaining the core cargo. During our preliminary emulsifier screening [12], poly (vinyl alcohol) (PVOH) was unsuccessful for retaining volatile heptane, but capsules indeed formed. Further investigations on its concen-tration effect followed, and heptane appeared to have been sealed when capsules were dispersed in water, indicated by a green fluo-rescent emission color with a fast retention inspection method [13], as demonstrated in Fig. 1(a). In all cases encaged heptane leaked out almost immediately upon drying of capsules from the aqueous phase, manifested by a red emission color (Fig. 1 (a), (b)). The fast release of heptane upon drying insinuated that the capsule shells were highly permeable to the volatile cargo and gen-uine retention of heptane was not achieved. Shell surface textures in some cases were grainy and patchy with pores residing within capsule shells, particularly at higher PVOH concentrations (Fig. 1 (c)). These open pores seemed to have occluded at lower PVOH concentrations (0.01 wt%). The orange-red emission colors from Fig. 1(a), nevertheless, implied that shell permeability was still too high for any meaningful retention of the cargo even in the absence of visible pores. Fig. 2 reveals the pores as viewed from inside the capsules. The grainy and patchy morphology disap-peared at a PVOH concentration of 0.002 wt% with only satellite particles being discretely lodged. However, formed capsules were extremely brittle and readily cracked or fragmented (Fig. 1(d)), again resulting in significant heptane leakage. At 0.5 wt%, no cap-sules were formed, and only precipitates were observed. This implied that the concentration of PVOH was probably too high to promote the deposition of molecular and particle aggregates onto

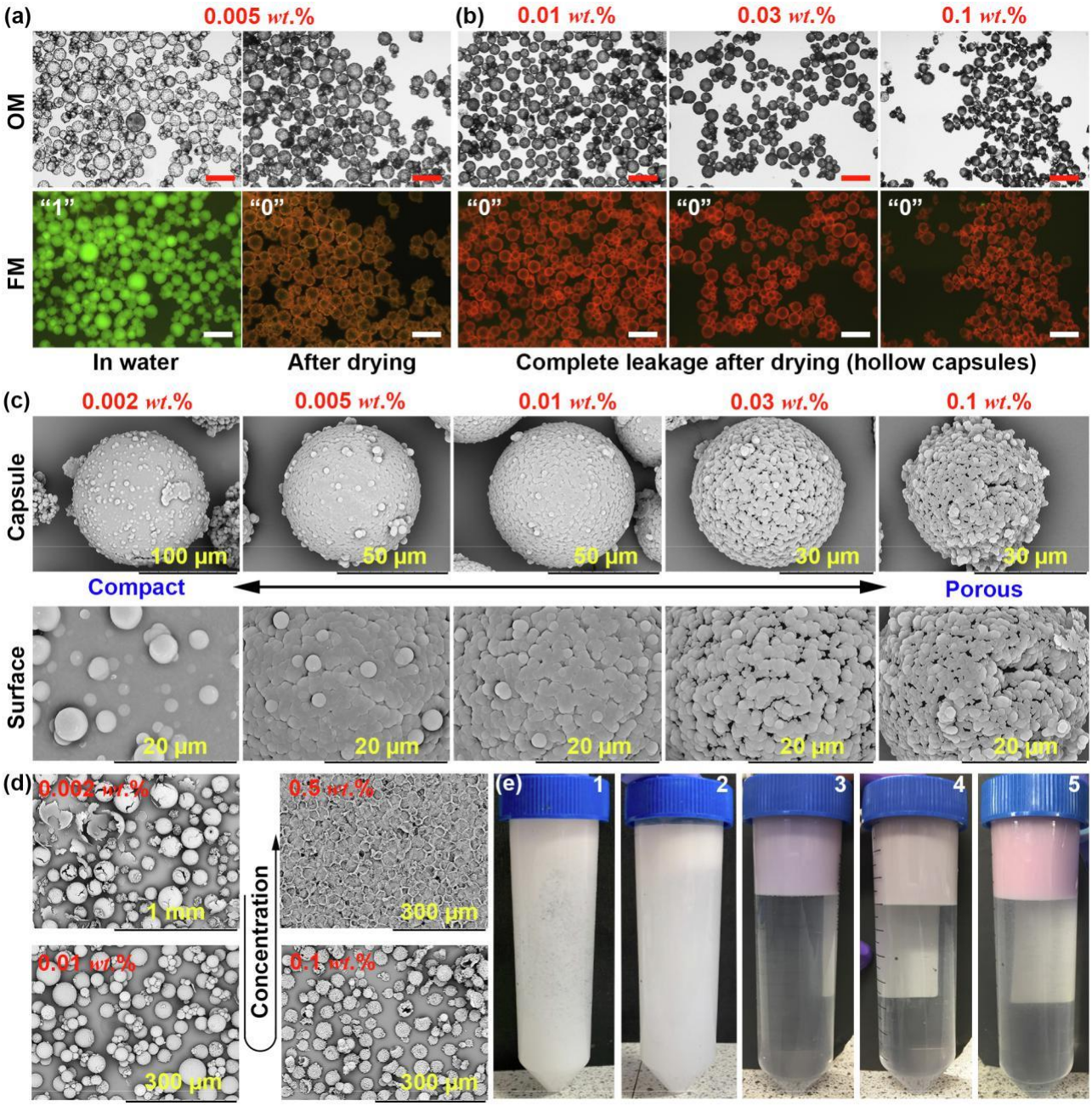

Fig. 1. (a) Bright-field (OM) and fluorescent microscopy (FM) images of capsules formulated with 0.005 wt% PVOH as the emulsifier. Heptane was retained inside capsules (indicated by a green emission color, denoted as ''1[00]) when they were dispersed inside water, but escaped immediately (indicated by a red emission color, denoted as ''0") upon capsule drying. All scale bars are 100 mm; (b) capsules formulated with 0.01, 0.03 and 0.1 wt% PVOH as the emulsifier showing complete heptane leakage upon capsule drying. All scale bars are 100 mm; (c) representative capsule surface morphology at various PVOH concentrations under scanning electron microscopy (SEM); (d) effect of PVOH concentration on capsule morphologies; (e) cloudy infranatant with dispersed PUF particles and floating capsules at the top from synthesis completed with (1) 0.02 wt
%XG and (2) 0.02 wt% MC, and clear infranatant without visible PUF particles and floating capsules at the top from synthesis completed with (3) 0.01 wt% (4) 0.03 wt% and (5)
0.05 wt% PVOH. All images were taken prior to centrifugation after the dispersion being allowed to settle for 5 min following transfer from the reactor.

the O/W interface for shell formation. Yoshizawa et al. claimed that no capsules formed when using PVOH as the emulsifier [16]. With-out any micrographs being provided, we presume that Yoshizawa et al. did not observe any capsule formation at a much higher poly-meric emulsifier concentration of 3.3 wt%, akin to our case of 0.5 wt%. In order to form capsules with PVOH as the emulsifier, a low concentration is preferred.

Soluble UF oligomers, insoluble molecular aggregates and parti-cle aggregates co-exist in the aqueous phase during synthesis of PUF resin [17]. Hydroxyls may have participated in the UF polycon-densation more slowly [3] than functional groups such as car-boxyls. It may also have improved the water solubility of molecular aggregates. Accordingly, PVOH is not able to serve as effective reaction foothold to form insoluble continuous PUF shells. It would only rely on the diffusion of insoluble particle aggregates to the O/W interface and their fusion to form capsule shells. If this process, somehow, is dominated by deposition of large-sized insol-uble particle aggregates onto the O/W interface, the interparticle gaps would grow in size which manifest themselves as pores in the shell structure. When shell formation is dominated by molec-

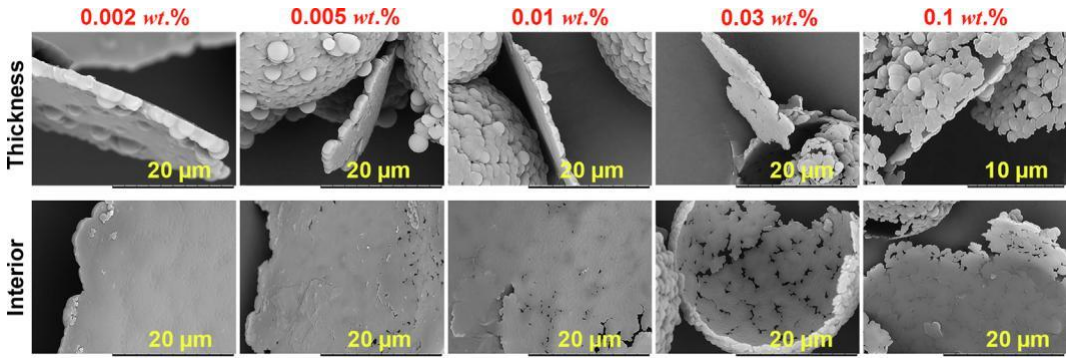

Fig. 2. Thickness and interior surface morphologies of capsule shells for miscellaneous PVOH concentrations.

ular aggregates smaller in size, the polymer structure would appear smooth with less visible pores. This implies that increasing PVOH could destabilize the insoluble molecular aggregates by increasing interparticle interactions and their tendency toward agglomeration into large particle aggregates. The abundant hydroxyls and corresponding hydrogen bonding as a result could easily promote such interparticle interactions.

Even though our initial attempt to use PVOH to encapsulate volatile heptane was unsuccessful, an important finding was dis-covered. PVOH, surprisingly, can substantially reduce sediment, which could potentially resolve the abovementioned issues. No sediment was observed inside the rather clear infranatant (Fig. 1
(e) 3-5) with naked eyes. Compared with this, the infranatant pro-duced with either methyl cellulose (MC) or xanthan gum (XG) as the emulsifier respectively was highly turbid with numerous dis-persed PUF precipitates (Fig. 1(e) 1-2). The sediment produced with either MC or XG was filtered, dried and weighed for calcula-tion. The sediment/precursors ratio was calculated by dividing sed-iment weight by the total weight of all precursors including urea, formaldehyde, resorcinol, ammonium chloride and emulsifier. The shell/precursors ratio was calculated by dividing shell product weight by the total weight of all precursors. Table 1 lists the calcu-lated results. No sediment could be filtered out when PVOH was used. However, the total shell product accounts for 75.8 ± 3.6%. This observation seems to suggest that PVOH promotes precipitate deposition at the O/W interface rather than its dispersion in the aqueous continuous phase.

3.2. Encapsulation with physically cross-linked PVOH via freeze-thawing

A large discrepancy in the Hansen solubility parameters (HSP) between capsule core and shell would lead to reduced shell perme-ability and inhibition of core diffusion [18]. Since heptane is a hydrocarbon and PVOH has plenty of hydroxyls, difference in the hydrogen bonding component (d_h) ($d_{h\ C7H16} = 0$) between the shell and core is expected to be large. If the pores, functioning as path-ways for small molecules to escape, are occluded within the shell polymer network, the abundant hydroxyls are expected to assist sealing heptane. Freeze-thawing cycles can physically cross-link PVOH and produce hydrogels [19–21]. This may increase the poly-mer density and reduce permeability. We therefore tested such modified PVOH as the emulsifier and results are presented in Fig. 3. Physical cross-linking of PVOH dramatically improved hep-tane retention in dry capsules, as opposed to immediate leakage in those synthesized with unmodified PVOH. Even though reten-tion was still far from being practically useful, this may provide a potential solution to improve the shell barrier properties if cross-linking PVOH can alter the density of the final polymer network.

Table 1
Sediment/precursors and shell/precursors ratios in capsule syntheses with 0.01% XG, MC and PVOH.

Emulsifier	Sediment/Precursors ratio	Shell/Precursors ratio
XG	25.5 ± 2.0%	2.5 ± 1.1%
MC	24.5 ± 1.6%	14.9 ± 3.1%
PVOH	0	75.8 ± 3.6%

3.3. Encapsulation with chemically cross-linked PVOH by PAA

Since physical cross-linking of PVOH reduced porosity within the PUF network, a more effective cross-linker is expected to fur-ther improve the retention. PAA has been reported as a cross-linker for PVOH [22–25]. PAA would promote polycondensation by participating in the reaction with its carboxyl moieties [16]. A

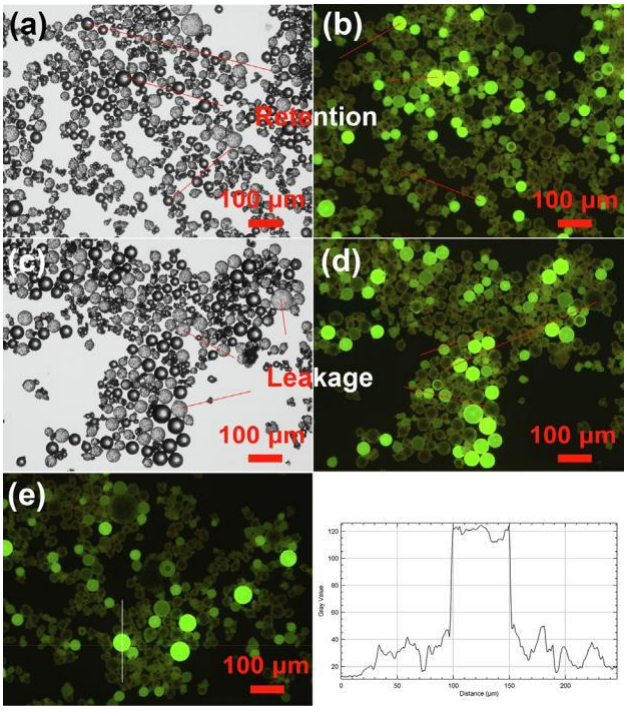

Fig. 3. (a–d) Heptane retention/leakage inspection at two randomly selected locations by the fluorescent staining method for capsules synthesized by physically cross-linked PVOH via freeze-thawing. Images were captured immediately after capsules were freshly dried from the aqueous dispersion medium. Bright green fluorescent color indicates heptane retention while dim green color implies leakage; (e) grey values along the white line drawn across both dim and bright fluorescent regions.

trade-off between the effects of PAA and PVOH on polycondensa-tion [3], and the cross-linking between these two molecules may be able to create a denser polymer structure to further improve capsule shell impermeability. Results in Fig. 4(a)–(d) revealed that cross-linking PVOH with PAA more successfully assisted in retain-ing heptane. Fig. 4(h) shows the payload evolution over 4 days after initial synthesis. Payload on the first day was calculated with the sample weight after fresh drying to be 67.5%. It should be noted, however, that the lower payload compared with benchmark capsules produced by gelatin (GEL) (>90%) [3] may not necessarily be because of potential leakage, but the core-shell ratio. The mean shell thickness was measured to be around 1.0 ± 0.1 mm, as opposed to 371 ± 10 nm for 0.01 wt% GEL. Payload dropped to 39.5% after 4 days, which was equivalent to 68.6% leakage. How-ever, for capsules produced by GEL, leakage was slow and on a much smaller order of magnitude (dashed line in Fig. 4(h)). Even though the long-term retention was still inferior to the benchmark capsules, our experiments indeed demonstrated a gradual improvement in capsule retention capability by physically and then chemically cross-linking PVOH. This opens up opportunities of investigating other potential cross-linkers for optimum retention.

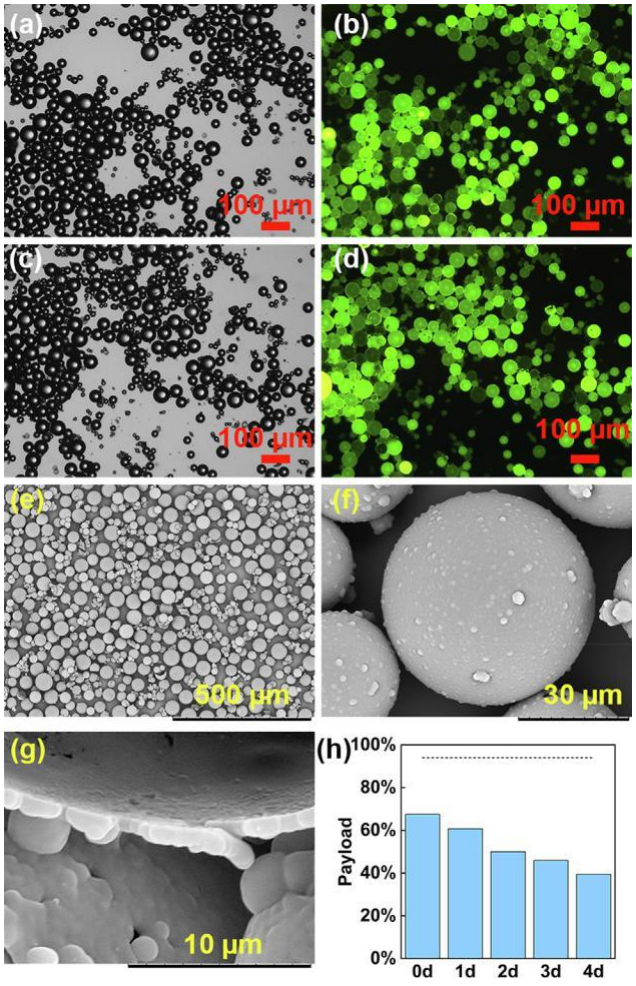

Fig. 4. (a),(c) Optical (b),(d) fluorescence microscopy of capsules synthesized via chemically cross-linking 0.01 wt% PVOH with 0.01 wt% PAA by heating the solution at 90 LC for 4 h. Images were captured immediately after capsules were freshly dried from water; (e-g) SEM micrographs of synthesized capsules and the cross section of a ruptured capsule; (h) payload of freshly dried capsules (PVOH + PAA) and their core leakage over 4 d. The reference dashed line represents the payload change for benchmark capsules produced with 0.01 wt% GEL as the emulsifier.

3.4. Mechanical properties of capsules

Using chemically cross-linked PVOH as the emulsifier seemed to have improved the mechanical strength of capsules compared to those produced by hydrocolloids. We could hardly compress some capsules synthesized by PAA cross-linked PVOH (PVOH + PAA) during micromanipulation with the same force transducer (403A, sensitivity 0.4529 mN/V, max load 4.5 mN) used previously for characterizing capsules formed with hydrocolloids

[3] before the maximum loading was quickly reached. A different transducer (400A, sensitivity 4.518 mN/V, max load 45 mN) was, therefore, employed. For the 30 capsules tested for each sample with either XG or MC as the emulsifier, all exhibited ultimate fail-ure under compression. The rupture percentage for capsules formed with GEL was 92%. However, when PVOH + PAA was used, only 14 capsules (<50%) showed ultimate failure as demonstrated in Fig. 5(a). more than 50% of the capsules exhibited no ultimate failure, but only yielding or pop-ins. Nominal rupture strain (29 ± 7%) was also higher than that of their counterparts (25 ± 3% for GEL, 19 ± 2% for XG and 24 ± 3% for MC). The Young's

modulus calculated by the Hertz equation [26,27] was 117 ± 33 MPa, which was higher than that of capsules formed with 0.01 wt% GEL (19 ± 3 MPa), XG (96 ± 12 MPa) or MC (57 ± 9 MPa) [3].

X-ray diffraction (Fig. 5(d)) identified only one prominent large broad peak around 19.2L and an almost indiscernible one around 42.1L when hydrocolloids were employed as the emulsifier. Using PVOH + PAA added an additional small peak on the diffractogram around 30.6L. We repeated XRD with 3 different batches and this small peak consistently appeared on all diffractograms. Prominent peaks around 31L and 40L have been reported for more crystalline PUF at lower formaldehyde/urea (F/U) molar ratios < 1.4 [28,29]. The crystallinity for such PUF resin was calculated to be 26% at a F/U molar ratio of 1.6 and shown to decrease with increasing F/U molar ratio [30]. The F/U molar ratio is approximately 2.0 in our recipe and the crystallinity would be lower. Since a single CAC bond is around 0.154 nm [31] and an amide bond has a length around 0.13 nm [32], PUF chain lengths should be typically

1 nm given that the degree of polymerization (DP) of polymers would normally be 10. HRTEM in Fig. 6 revealed no orderly structures within capsule shells on such a length scale. It is postu-lated that PUF shells at least do not present long-range order. The inset in Fig. 6 corresponds to the fast Fourier transform (FFT) of the highlighted areas and shows diffuse rings indicative of amorphous materials with little or no periodicity. Consequently, it is believed that PUF capsule shells are very likely amorphous. However, the new peaks on XRD diffractograms of capsule shells formed with PVOH + PAA and the less diffuse ring pattern from FFT implicate that such an emulsifier may have modified the short-range order of polymer chains. It is also worth noting that the shell thickness seen in Fig. 6 is in keeping with the average measurements previ-ously determined by SEM.

Increasing Young's modulus of capsules could be caused by either increasing shell thickness from sub-microns (371 ± 10 nm for 0.01 wt% GEL, 823 ± 15 nm for 0.01 wt% XG and 662 ± 12 nm for 0.01 wt% MC) [3] to 1.0 ± 0.1 mm, or modification in polymer crystallinity. We have confirmed the former with all three hydro-colloids previously [3]. Characterization of the batch synthesized by cross-linking 0.01 wt% PVOH with 0.01 wt% PAA at 90 LC for 12 h revealed that capsules had a mean shell thickness of 267 ± 18 nm and the Young's modulus was 52 ± 5 MPa (Fig. 5(c)).

If the different mechanical properties were entirely caused by shell thickness effect, the micrometer-shelled capsules would have been more brittle than those produced by 0.01 wt% XG. An increas-ing nominal rupture strain and lowering fracture percentage of these capsules suggest improvement in shell plasticity in addition

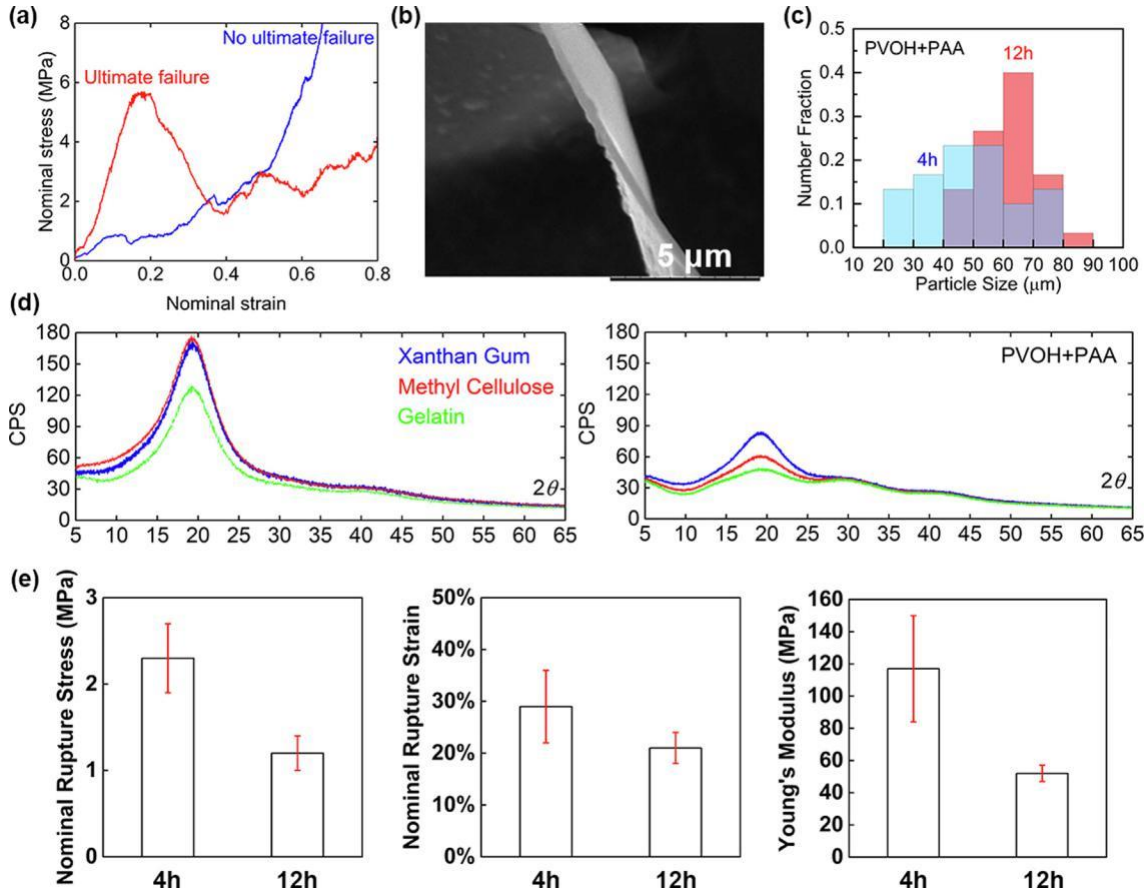

Fig. 5. (a) Typical loading characteristics of capsules produced by PVOH + PAA as the emulsifier. The red curve shows capsule undergoing ultimate failure, while the blue curve represents one exhibiting no ultimate failure but yielding and pop-ins; (b) a SEM image showing the cross section of a ruptured capsule synthesized by PVOH + PAA at 90 LC for 12 h; (c) particle size distribution of capsules synthesized by PVOH + PAA at 90 LC for 4 and 12 h; (d) x-ray diffraction (XRD) diffractograms of capsules produced by MC, XG, GEL and PVOH + PAA (3 replicates); (e) the Young's modulus, nominal rupture stress and nominal rupture strain of capsules synthesized with PVOH + PAA at 90 LC for 4 and 12 h.

to the Young's modulus increase. The plasticity improvement is believed to be attributed to PVOH + PAA in this case possibly via hydrogen bonding from the abundant hydroxyls.

3.5. Graphene-oxide impregnation

Another appealing advantage of using PVOH (or PVOH + PAA) emerged while we were attempting to imbed graphene oxide (GO) inside the PUF capsule shell for barrier and thermal property improvement. We dispersed GO in the aqueous phase and initiated the polymerization in order to synthesize PUF shells with GO. Sur-prisingly, we noticed that the majority of GO migrated into cap-sules after synthesis rather than being suspended in water. This was implicated by the observation that the aqueous dispersions were very dark before emulsification, while dark-colored capsules floated on the top after synthesis due to their lower density leaving the translucent infranatant without a dark tone (Fig. 7(a) and (b)). Since there was barely any sedimentation, GO did not end up sub-stantially as sediment either. Such a peculiar binding ability of PVOH to GO translates into a very high utilization rate of the expensive material. The shell material, PUF, with and without GO was pressed into tablets for Raman spectroscopy in order to further prove GO impregnation in capsules. PUF exhibited three large peaks at 1307, 1446 and 1625 cm ^{1}, corresponding to twisting of $A(CH_2)_nA$ ($n > 3$), bending of methylene in ACH_2AOH, and amide carbonyls, respectively (Fig. 6(d)) [33,34]. GO showed the D band at 1321 cm ^{1} and the G band at 1608 cm ^{1} [35]. When the shell material is composed of both PUF and GO, all characteristic peaks superimposed into a single broad one.

GO has shown certain amphiphilic surface activities for emul-sion stabilization via Pickering effect [36], and would compete with PVOH for adsorption at the O/W interface. Nevertheless, GO is believed to possess very low emulsification efficiency for nonaro-matic nonpolar oils such as aliphatic hydrocarbons due to the lack of p-p interactions [37]. PVOH, on the other hand, has a high hydrophilic-lipophilic balance (HLB) value of 18 [38], good for sta-bilizing O/W emulsions [39]. Therefore, PVOH is likely to have a stronger affinity towards the O/W interface for stabilizing emul-sion drops. Nevertheless, abundant hydroxyls and epoxide groups are available on its basal plane and carboxyl moieties are around the edges of the flake [40,41]. Carboxyl groups have been used for cross-linking with PVOH [22–25] and participating in the UF polycondensation reaction [15]. Even though PVOH is preferen-tially adsorbed at the interface, GO flakes are able to migrate to the interfacial region to impregnate into PUF shell owing to its abil-ity to cross-link with PVOH by the edge carboxyl moieties. Further cross-linking of GO within the PUF polymer network is also possi-ble with carboxyl groups on the edges of GO reacting with the methylol group [15].

For the purpose of demonstrating that this binding behavior is unique to PVOH among all emulsifiers tested in this work, we tested GEL and MC as the co-emulsifier with GO. Both batches of syntheses produced sediment, contrary to when PVOH was used (Fig. 7(f) and (g)). We compared the colors first between dried

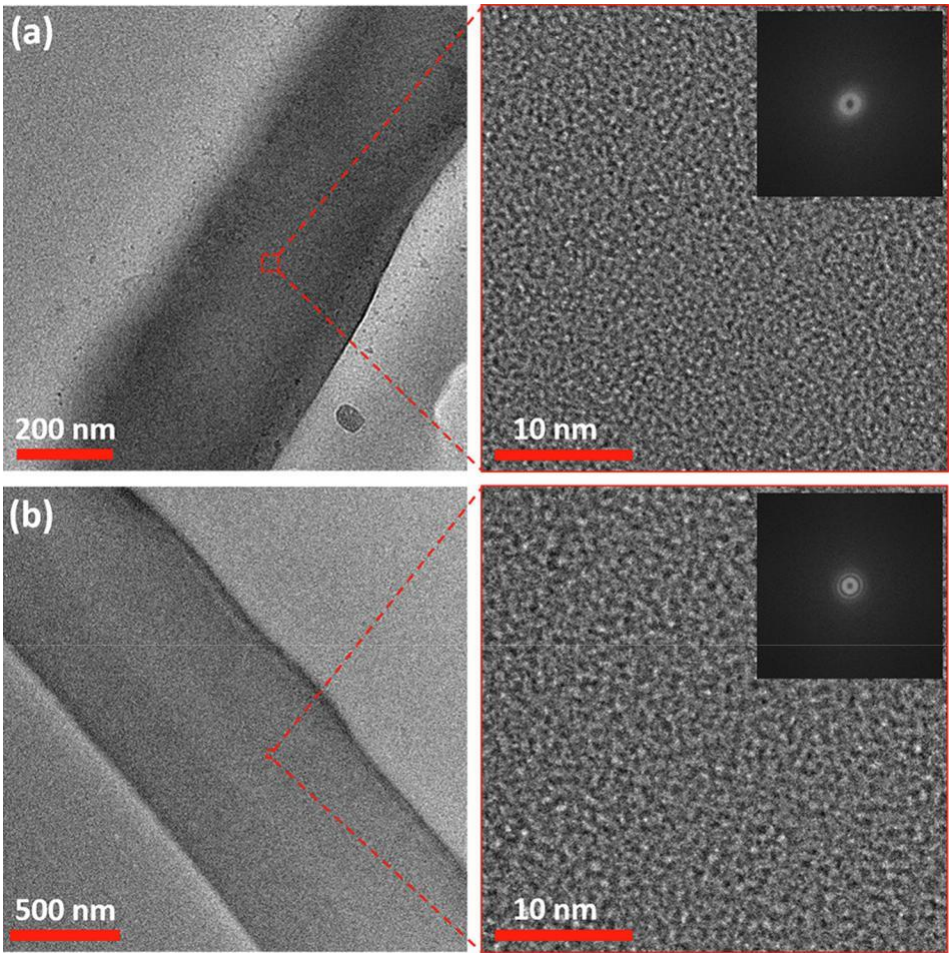

Fig. 6. TEM images of PUF shells formed by using (a) GEL and (b) PVOH + PAA as the emulsifier. High resolution images of the highlighted areas are shown with the FFT inset.

capsules and sediment. For the batch formulated with MC, the col-ors of both capsules and sediment appeared to be similar, which implied that GO could be present in both. When GEL was used, the color of sediment was darker than capsules, indicating that GO might be predominantly imbedded inside sediment rather than in capsules. Raman spectra of sediment in Fig. 7(h) confirmed that GO were indeed present in sediment for both batches.

4. Conclusions and future perspectives

In this work, we succeeded in using PVOH as an emulsifier [12,16] for encapsulating a challenging volatile cargo via one-step in situ polymerization. Even though PVOH was cross-linked by carboxylic groups to make retention possible, previous effort has demonstrated that carboxyl or anhydride moieties are not nec-essary [3,12] as opposed to the prevalent usage of carboxyl-bearing emulsifiers [6,16,33,42–45]. If there is no chemical reaction between the emulsifier and monomers, or the reaction rate is low, preferentially adsorbed emulsifiers could not expand a contin-uous shell growth from chemical reactions initiating from such functional groups. Shell formation is predominantly determined by diffusion of insoluble particle aggregates onto the O/W inter-face. When such aggregates grow to a certain size range, shell structures become porous due to interparticle gaps. In order to retain volatile cargos with PVOH, a low concentration is preferred with a cross-linker promoting chemical reactions. Cross-linking the polymer network would close pores and increase its density to block leakage of small molecules. The most significant merit of using PVOH as the emulsifier to synthesize capsules is the substan-tial reduction of PUF precipitates usually produced during in situ polymerization, which eliminates the need for centrifugation to harvest capsules. Such an improvement foresees a huge industrial benefit in terms of reducing production time and simplifying man-ufacturing procedures. Meanwhile, capsules produced with the PVOH emulsifier also demonstrate stronger mechanical properties in terms of Young's modulus and nominal rupture strain. This is likely caused by thicker shells and a localized short-range order change. Interestingly, we also discovered that PVOH facilitated binding of GO into capsules likely owing to its binding abilities via chemical reactions. This features a high utilization efficiency of the expensive functional materials. In order to validate the hypothesis from a chemical reaction point of view, reaction rates of various functional groups such as carboxyls, hydroxyls, amines and amides in the UF polycondensation should be studied.

Declaration of Competing Interest

The authors declare that they have no known competing finan-cial interests or personal relationships that could have appeared to influence the work reported in this paper.

Acknowledgement

The authors give their special thanks to the Engineering and Physical Sciences Research Council (EPSRC) in the United Kingdom for the funding provided to this project (EP/N000714/1 and EP/

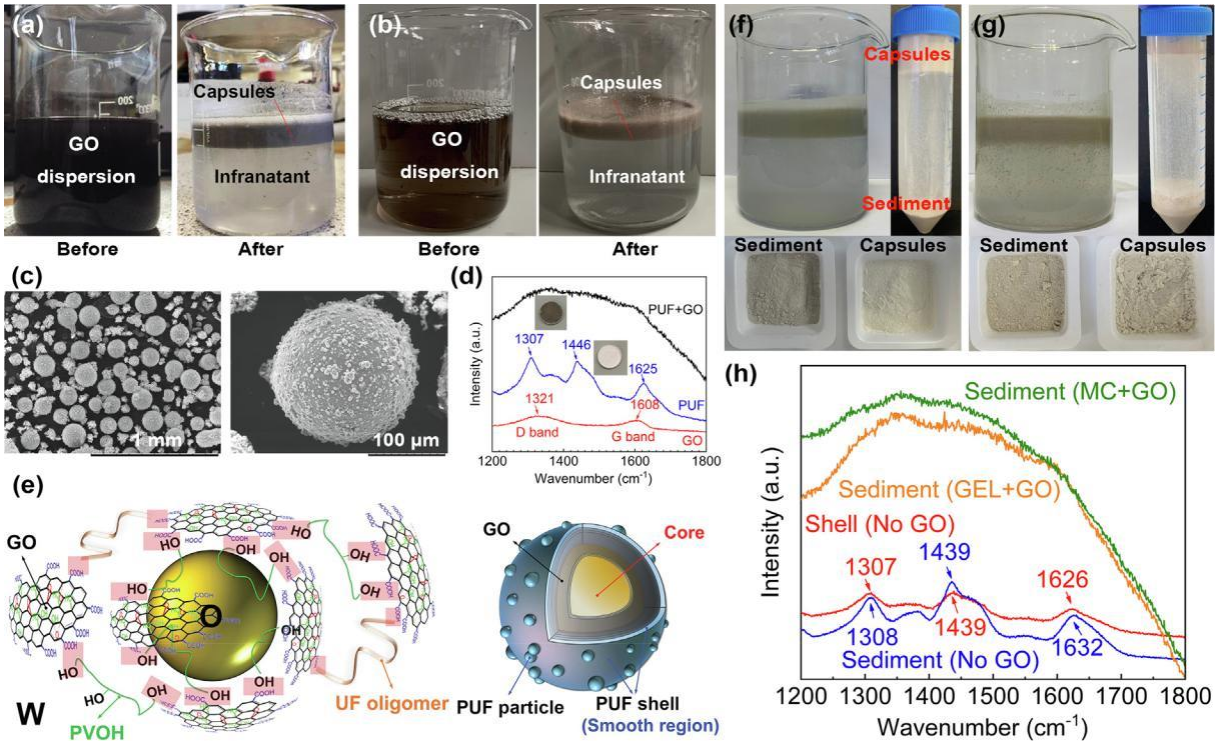

Fig. 7. GO dispersion before emulsification and GO accumulation within capsules after synthesis without centrifugation with (a) 0.01 wt% PVOH and (b) 0.01 wt% PVOH cross-linked with 0.01 wt% PAA as the emulsifier; (c) SEM micrographs of capsules formed with GO and 0.01 wt% PVOH cross-linked with 0.01 wt% PAA; (d) Raman spectra of pure GO, PUF shell and PUF + GO; (e) a schematic illustration of the intercarlation between PVOH, GO and UF oligomers forming the capule shell. Pink squares represent the cross-linking sites between GO and UF oligomers and PVOH; (f) suspension of capsules and sediment in a beaker settling for 5 min after synthesis with 0.01 wt% GEL and GO before centrifugation; capsules on the top and sediment at the bottom of a tube after centrifugation of the suspension; dried and separated sediment and capsules; (g) suspension of capsules and sediment in a beaker settling for 5 min after synthesis with 0.01 wt% MC and GO before centrifugation; capsules on the top and sediment at the bottom of a tube after centrifugation of the suspension; dried and separated sediment and capsules; (h) Raman spectra of PUF shell and sediment without GO, and sediment from syntheses by GEL + GO and MC + GO.

N021142/1). The authors would like to thank Mrs Theresa Morris from the School of Metallurgy and Materials at the University of Birmingham for TEM sample preparation, as well as the Cardiff University electron microscopy facility for the TEM experiments completed.

References

[1] J.P. Hitchcock, A.L. Tasker, E.A. Baxter, S. Biggs, O.J. Cayre, Long-term retention of small, volatile molecular species within metallic microcapsules, ACS Appl. Mater. Interfaces 7 (27) (2015) 14808–14815.
[2] H. Liu, X. Wang, D. Wu, Innovative design of microencapsulated phase change materials for thermal energy storage and versatile applications: a review, Sustain. Energy Fuels 3 (5) (2019) 1091–1149.
[3] Y. Zhang, D. Baiocco, A.N. Mustapha, X. Zhang, Y. Qinghua, G. Wellio, Z. Zhang, Y. Li, Hydrocolloids: nova materials assisting encapsulation of volatile phase change materials for cryogenic energy transport and storage, Chem. Eng. J. 382 (2020) 123028.
[4] K. Dietrich, H. Herma, R. Nastke, E. Bonatz, W. Teige, Amino resin microcapsules. I. Literature and patent review, Acta Polym. 40 (4) (1989) 243–251.
[5] E.N. Brown, S.R. White, N.R. Sottos, Microcapsule induced toughening in a self-healing polymer composite, J. Mater. Sci. 39 (5) (2004) 1703–1710.
[6] B.J. Blaiszik, M.M. Caruso, D.A. McIlroy, J.S. Moore, S.R. White, N.R. Sottos, Microcapsules filled with reactive solutions for self-healing materials, Polymer 50 (4) (2009) 990–997.
[7] T. Nesterova, K. Dam-Johansen, S. Kiil, Synthesis of durable microcapsules for self-healing anticorrosive coatings: a comparison of selected methods, Progr. Organic Coat. 70 (4) (2011) 342–352.
[8] Z. Chen, J. Wang, F. Yu, Z. Zhang, X. Gao, Preparation and properties of graphene oxide-modified poly(melamine-formaldehyde) microcapsules containing phase change material n-dodecanol for thermal energy storage, J. Mater. Chem. A 3 (21) (2015) 11624–11630.
[9] G. Fang, H. Li, F. Yang, X. Liu, S. Wu, Preparation and characterization of nano-encapsulated n-tetradecane as phase change material for thermal energy storage, Chem. Eng. J. 153 (1) (2009) 217–221.
[10] O. Nguon, F. Lagugné-Labarthet, F.A. Brandys, J. Li, E.R. Gillies, Microencapsulation by in situ polymerization of amino resins, Polym. Rev. (2017) 1–50.
[11] W. Sliwka, Microencapsulation, Angew. Chem., Int. Ed. Engl. 14 (8) (1975) 539–550.
[12] Y. Zhang, Z. Jiang, Z. Zhang, Y. Ding, Q. Yu, Y. Li, Polysaccharide assisted microencapsulation for volatile phase change materials with a fluorescent retention indicator, Chem. Eng. J. 359 (2019) 1234–1243.
[13] Y. Zhang, Z. Zhang, Y. Ding, Z. Pikramenou, Y. Li, Converting capsules to sensors for nondestructive analysis: from cargo-responsive self-sensing to functional characterization, ACS Appl. Mater. Interfaces 11 (9) (2019) 8693–9642.
[14] Z. Zhang, Mechanical strength of single microcapsules determined by a novel micromanipulation technique, J. Microencapsul. 16 (1) (1999) 117–124.
[15] S. Peker-Baslara, B. Övez, Ö. Balcioğlu, Properties of gelatin-gum arabic coacervates composited with amino resins, J. Chem. Technol. Biotechnol. 56 (2) (1993) 175–184.
[16] H. Yoshizawa, E. Kamio, E. Kobayashi, J. Jacobson, Y. Kitamura, Investigation of alternative compounds to poly(E-MA) as a polymeric surfactant for preparation of microcapsules by phase separation method, J. Microencapsul. 24 (4) (2007) 349–357.
[17] J.M.M. Ferra, A.M. Mendes, M.R.N. Costa, L.H. Carvalho, F.D. Magalhães, A study on the colloidal nature of urea-formaldehyde resins and its relation with adhesive performance, J. Appl. Polym. Sci. 118 (4) (2010) 1956–1968.
[18] I. Hofmeister, K. Landfester, A. Taden, Controlled formation of polymer nanocapsules with high diffusion-barrier properties and prediction of encapsulation efficiency, Angew. Chem. Int. Ed. 54 (1) (2015) 327–330.
[19] C.M. Hassan, N.A. Peppas, Structure and morphology of freeze/thawed PVA hydrogels, Macromolecules 33 (7) (2000) 2472–2479.
[20] R. Ricciardi, F. Auriemma, C. De Rosa, Structure and properties of poly(vinyl alcohol) hydrogels obtained by freeze/thaw techniques, Macromol. Symp. 222 (1) (2005) 49–64.
[21] J.L. Holloway, A.M. Lowman, G.R. Palmese, The role of crystallization and phase separation in the formation of physically cross-linked PVA hydrogels, Soft Matter 9 (3) (2013) 826–833.
[22] L.F. Gudeman, N.A. Peppas, Preparation and characterization of pH-sensitive, interpenetrating networks of poly(vinyl alcohol) and poly(acrylic acid), J. Appl. Polym. Sci. 55 (6) (1995) 919–928.
[23] K. Kumeta, I. Nagashima, S. Matsui, K. Mizoguchi, Crosslinking reaction of poly (vinyl alcohol) with poly(acrylic acid) (PAA) by heat treatment: effect of neutralization of PAA, J. Appl. Polym. Sci. 90 (9) (2003) 2420–2427.
[24] G.A. Gaddy, A.S. Korchev, J.L. McLain, B.L. Slaten, E.S. Steigerwalt, G. Mills, Light-induced formation of silver particles and clusters in crosslinked PVA/PAA films, J. Phys. Chem. B 108 (39) (2004) 14850–14857.
[25] H. Byun, B. Hong, S.Y. Nam, S.Y. Jung, J.W. Rhim, S.B. Lee, G.Y. Moon, Swelling behavior and drug release of poly(vinyl alcohol) hydrogel cross-linked with poly(acrylic acid), Macromol. Res. 16 (3) (2008) 189–193.

[26] K.L. Johnson, Contact Mechanics, Cambridge University Press, Cambridge, United Kingdom, 1985.
[27] L. Kuo-Kang, Deformation behaviour of soft particles: a review, J. Phys. D Appl. Phys. 39 (11) (2006) R189.
[28] B.-D. Park, H.-W. Jeong, Hydrolytic stability and crystallinity of cured urea–formaldehyde resin adhesives with different formaldehyde/urea mole ratios, Int. J. Adhes. Adhes. 31 (6) (2011) 524–529.
[29] M. Liu, R.V.K.G. Thirumalai, Y. Wu, H. Wan, Characterization of the crystalline regions of cured urea formaldehyde resin, RSC Adv. 7 (78) (2017) 49536–49541.
[30] B.-D. Park, V. Causin, Crystallinity and domain size of cured urea– formaldehyde resin adhesives with different formaldehyde/urea mole ratios, Eur. Polym. J. 49 (2) (2013) 532–537.
[31] L.S. Bartell, On the length of the carbon-carbon single bond1, J. Am. Chem. Soc. 81 (14) (1959) 3497–3498.
[32] Frank H. Allen, Olga Kennard, David G. Watson, Lee Brammer, A. Guy Orpen, Robin Taylor, Tables of bond lengths determined by X-ray and neutron diffraction. Part 1. Bond lengths in organic compounds, J. Chem. Soc., Perkin Trans. 2 (12) (1987) S1, https://doi.org/10.1039/p298700000s1.
[33] S. Cosco, V. Ambrogi, P. Musto, C. Carfagna, Properties of poly(urea-formaldheyde) microcapsules containing an epoxy resin, J. Appl. Polym. Sci. 105 (3) (2007) 1400–1411.
[34] P. Larkin, Chapter 6 - IR and Raman spectra-structure correlations: characteristic group frequencies, in: Infrared and Raman Spectroscopy, Elsevier, Oxford, 2011, pp. 73–115.
[35] A.M. Giuliodori, A. Brandi, S. Kotla, F. Perrozzi, R. Gunnella, L. Ottaviano, R. Spurio, A. Fabbretti, Development of a graphene oxide-based assay for the sequence-specific detection of double-stranded DNA molecules, PLoS ONE 12 (8) (2017) e0183952.
[36] F. Kim, L.J. Cote, J. Huang, Graphene oxide: surface activity and two-dimensional assembly, Adv. Mater. 22 (17) (2010) 1954–1958.
[37] Y. He, F. Wu, X. Sun, R. Li, Y. Guo, C. Li, L. Zhang, F. Xing, W. Wang, J. Gao, Factors that affect pickering emulsions stabilized by graphene oxide, ACS Appl. Mater. Interfaces 5 (11) (2013) 4843–4855.
[38] Q. Xu, A. Crossley, J. Czernuszka, Preparation and characterization of negatively charged poly(lactic-co-glycolic acid) microspheres, J. Pharm. Sci. 98 (7) (2009) 2377–2389.
[39] Yan Zheng, Minying Zheng, Zonghui Ma, Benrong Xin, Ruihua Guo, Xuebing Xu, Sugar fatty acid esters, in: Polar Lipids, Elsevier, 2015, pp. 215–243, https://doi.org/10.1016/B978-1-63067-044-3.50012-1.
[40] W. Cai, R.D. Piner, F.J. Stadermann, S. Park, M.A. Shaibat, Y. Ishii, D. Yang, A. Velamakanni, S.J. An, M. Stoller, J. An, D. Chen, R.S. Ruoff, Synthesis and solid-state NMR structural characterization of ^{13}C-labeled graphite oxide, Science 321 (5897) (2008) 1815–1817.
[41] O.C. Compton, D.A. Dikin, K.W. Putz, L.C. Brinson, S.T. Nguyen, Electrically conductive ‘‘alkylated” graphene paper via chemical reduction of amine-functionalized graphene oxide paper, Adv. Mater. 22 (8) (2010) 892–896.
[42] E.N. Brown, M.R. Kessler, N.R. Sottos, S.R. White, In situ poly(urea-formaldehyde) microencapsulation of dicyclopentadiene, J. Microencapsul. 20 (6) (2003) 719–730.
[43] H. Yoshizawa, E. Kamio, N. Hirabayashi, J. Jacobson, Y. Kitamura, Membrane formation mechanism of cross-linked polyurea microcapsules by phase separation method, J. Microencapsul. 21 (3) (2004) 241–249.
[44] C. Fan, X. Zhou, Effect of emulsifier on poly(urea–formaldehyde) microencapsulation of tetrachloroethylene, Polym. Bull. 67 (1) (2011) 15–27.
[45] S. Cosco, V. Ambrogi, P. Musto, C. Carfagna, Urea-formaldehyde microcapsules containing an epoxy resin: influence of reaction parameters on the encapsulation yield, Macromol. Symp. 234 (1) (2006) 184–192.